J Inorg Organomet Polym (2014) 24:515–524
DOI 10.1007/s10904-013-0004-x

Ultra-Fine Characteristics of Starch Nanoparticles Prepared Using Native Starch With and Without Surfactant

A. Hebeish · M. H. El-Rafie · M. A. EL-Sheikh · Mehrez E. El-Naggar

Received: 24 September 2013 / Accepted: 11 November 2013 / Published online: 26 November 2013

Abstract Starch nanoparticles (St-NPs) were synthesized using native maize starch (NS). The synthesis was carried out as per the Solvent displacement method after being modified. Modification involved the use of aqueous alkaline medium as the solvent and ethanol as the organic non-solvent. This was done with a view to assure easier and more reproducible St-NPs preparation without consuming more solvent. The modified method for preparation of St-NPs was evaluated; investigation into factors affecting it were made in order to discover the optimum conditions for such preparation. Factors studied included concentration of starch as well as concentration of surface-active agent, namely, Tween® 80, which was added before precipitation. World-class facilities was used for evaluation of the obtained St-NPs such as transmission electron microscopy, particle size analyzer, polydispersity index (PdI), Fourier transform infrared (FT-IR) spectroscopy and, X-ray diffraction. The results indicate that there are no changes of the chemical structure of St-NPs as indicated by FT-IR and the crystallinity pattern is converted from A-type to amorphous (V-type). The data obtained indicate also that the smallest, highly distributed particles size with good PdI of St-NPs are obtained in the presence of 20 % Tween® 80 (based on weight of NS).

Keywords Solvent displacement method · Alkali dissolved starch · Starch nanoparticles

A. Hebeish · M. H. El-Rafie · M. A. EL-Sheikh · M. E. El-Naggar (✉)
Textile Research Division, National Research Centre, Dokki, Cairo, Egypt
e-mail: mehrez_chem@yahoo.com

1 Introduction

One of the biggest challenges of science and technology today is to control polymer size and morphology at the nanometer state. Up to date, there is no universally accepted size range that particles must have to be classified as microparticles or nanoparticles. However, many researchers classify particles smaller than 1 μm as nanoparticles and particles larger than 100 mm as macroparticles [1]. Nanoparticles are then submicronic colloidal system, ranging in size from a few nanometers to 1 μm, made of artificial or natural polymers [2]. Nanoscale typically has greater surface area per mass. The nanometric size effect have led to intensive research in the area of nano-sized particles [3, 4] from natural polysaccharide polymers such as cellulose, [5, 6] chitin, [7] and starch [3, 4, 8–16].

Starch nanoparticles (St-NPs) have attracted much attention due to their unique properties that are different significantly from their bulk materials [17]. Starch nanocrystals have been extracted from starch granules by means of physical or chemical treatments. Utilization of chemical treatments for preparation of St-NPs has more attention than physical treatments [18].

The extraction of starch nanocrystals have been the subject of numerous reports [14, 18–23]. The main approach adopted to produce starch nanocrystals is based on the use of acid hydrolysis to dissolve the amorphous and paracrystalline regions of the starch granules [10, 23]. The ensuing nanoparticles are parallel shaped nanoplatelets around 5–7 nm thick, 20–40 nm long and 15–30 nm wide. However, the main drawbacks of such a method remained the long duration, along with the low yield being in the range of 2–15 %.

The isolation of starch using high-pressure homogenization was report for the production of St-NPs this method

leads to crystalline microparticles, which turn, into amorphous nanoparticles by increasing run numbers in water/oil (W/O) system in the presence of more than one surfactant as well as crosslinking agent at high temperature [24].

It was also reported that St-NPs could be synthesized by precipitating soluble starch solution in absolute ethanol under controlled conditions in presence of urea as stabilizing agent. The main drawbacks of such a method are that it is not economical due to: (a) the large amount of solvent used for precipitation and (b) the preparation method did not allow proper control of particle sizes. As a result, main particle size remained large (between 400 and 600 nm) [17, 25].

Environmentally friendly mechanical approach was the subject of two patents [26, 27] for producing St-NPs less than 400 nm in size. The process is based on reactive extrusion of cross-linked plasticized starch followed by grinding and high-speed dispersion in water.

Solvent displacement method is one of the methods used for synthetic and natural polymer nanoparticles preparations [28–31]. It was first developed by Fessi et al. [32] as simple and reproducible process. Nano-precipitation occurs instantaneously when the primary solution is added drop wise to the non-solvent phase.

In the present work, St-NPs are synthesized using native starch. The Solvent displacement method is modified by using aqueous alkaline medium as the solvent and ethanol as the organic non-solvent with the anticepitation that this modification may lead to an easier and more reproducible St-NPs without consuming more solvent. Factors affecting the synthesis of St-NPs are studied including the effect of NS concentration and the concentration of the surface-active agent added to the starch dispersion before precipitation. State-of-the-art facilities such as transmission electron microscopy (TEM), particle size analyser, polydispersity index (PdI), Fourier transform infrared (FT-IR) spectroscopy and X-ray diffraction (XRD) are employed for studying the characterization and properties of nano-sized starch particles.

2 Materials and Methods

2.1 Materials

Native maize starch (NS) was supplied by the Egyptian Company for Starch and Glucose Manufacture, Cairo, Egypt.

Tween® 80 (polysorbate 80) >99.9 % was obtained from Sigma Chemical Co. USA. Sodium hydroxide and absolute ethyl alcohol were of analytical grade and used without further purification.

2.2 Methods

2.2.1 Preparation of St-NPs

Different amounts of dried NS (2.5, 5, 7.5 and 10 g) were added independently to 100 ml H_2O containing 1.5 g sodium hydroxide which was used as a solvent system. The mixture was kept for 120 min at 25 °C under continuous mechanical stirring until formation of homogeneous gelatinized maize starch. Then, 100 ml of absolute ethanol were added drop wise to the gelatinized starch solution under vigorous mechanical stirring. The resulting St-NPs suspension was centrifuge at 4,500 rpm for 30 min. The supernatant was removed and the settled St-NPs obtained from the centrifugation process were further purified by using twice 80/20 ethanol/water and finally washed with absolute ethanol to remove water and unreacted components.

2.2.2 Freeze-drying of nanoparticles

The resulting solution of St-NPs was freeze-dried using a freeze dryer [13]. Freezing was the first step of freeze-drying. During this step, the liquid suspension of St-NPs was cooled at −60 °C for 6 h and ice crystals of pure water were formed. The primary drying stage involves sublimation of ice from the frozen product at 0.07 mbar pressure at −60 °C for 8 h, and secondary drying involved the removal of absorbed water from the product at 25 °C for 2 h. The obtained freeze-dried St-NPs were used for testing and analysis.

After evaluation of the resultant St-NPs, the effect of incorporation of different concentration of surface-active agent (Tween® 80) in the preparation medium was also studied.

2.3 Characterization and Properties

2.3.1 Transmission Electron Microscopy

The morphological examination of the nanoparticles was performed by TEM on a JEOL (JEM-1230) Japan. Instrument with an acceleration voltage of 120 kV. The sample for TEM analysis was obtained by placing a drop of the colloid dispersion onto a carbon coated copper grid. The samples dried at room temperature were then examined using a TEM without further modification or coating. The particle size distribution of the Ag NPs obtained from TEM images were measured using Image J 1.45 s software, accurately by choosing at least 100 particles from different TEM micrographs.

2.3.2 Particle Size Analysis (PS)

The average size and size distribution of the nanoparticles were estimated by dynamic light scattering (DLS) using a

Malvern Zetasizer Nano (Malvern Instruments Ltd., UK) equipped with a He–Ne laser (0.4 mW; 633 nm) and a temperature-controlled cell holder. The intensity of the scattered light was detected at 90° to the incident beam. The measurements were performed in samples diluted in Milli Q water and analyzed at 25 °C [33]. The mean intensity-weighted diameter was recorded as the average of three measurements.

2.3.3 Polydispersity Index

Polydispersity Index is a parameter used to define the particle size distribution of nanoparticles obtained from DLS. Its dimensionless number is extrapolated from the autocorrelation function and PdI ranges from a value 0.1–0.5 for suitable measurements and good-quality of the colloidal suspensions to values close to one for poor-quality samples, which has a very broad size distribution and may contain large particles or aggregates [34].

2.3.4 Fourier Transform Infrared (FTIR) Spectroscopy

FT-IR spectra were recorded for NS and St-NPs on Perkin-Elmer spectrum 1000 spectrophotometer. The sample (0.02 g) was mixed with KBr to form a round disk suitable for FT-IR measurements. The IR spectra were scanned over the wave number range of 4,000–400 cm^{-1}.

2.3.5 X-ray diffraction (XRD)

X-ray diffraction patterns of finely powdered samples were recorded on a Philips PW3040 X-ray diffractometer system by monitoring the diffraction angle from 5° to 80° (2θ) at 40 keV.

3 Results and Discussion

Native starch (NS) granules are polygonal with a smooth surface, about 2–20 μm in size when evaluated using SEM. Starch molecules contain 30–35 % amylose (linear molecules) and 65–70 amylopectin (branch molecules) makes these molecules insoluble in water. After adding NS to sodium hydroxide solution, the bonding interaction between starch molecules including hydrogen bond in swollen state was broken by strong mechanical stirring. In this way, the small particles were split away from each other at room temperature without raising temperature.

3.1 Factors Affecting Synthesis of St-NPs Using NS

Optimum conditions for the preparation of St-NPs could be achieved through studying the effect of concentration of NS and the surface-active agent on the characteristics of St-NPs as given below.

3.1.1 Native Starch (NS) Concentration

Different concentrations of NS (2.5, 5, 7.5, 10 %) were dissolved in sodium hydroxide solution followed by addition of absolute ethanol to the gelatinized maize starch solution as described in the experimental section.

Figures 1–4 depicts the morphology as visualized by TEM, PdI and particle size as measured by particle size analyzer of St-NPs using the aforementioned concentrations.

As is evident from Fig. 1a–c using 2.5 % NS leads to the formation of good spherical nanoparticles with particle size ranging between 40 and 190 nm. But with the capacity that the majority of nanoparticles acquire an average size of 132 nm with PdI equal 0.4 as shown in Fig. 1c. Increasing NS concentration to 5 % leads to the formation of St-NPs which still have definite spherical shape and no conglomeration but with marginal increment in the nanoparticle size which ranges from 135 to 155 nm (Fig. 2a, b). Meanwhile the particle size analyzer refers to a value of 164 nm and PdI of 0.333 as shown in Fig. 2c, Increasing NS up to 7.5 % gives highly aggregated St-NPs (Fig. 3a) and the particle size analyzer gives a value of 220 nm with PdI equal to 0.747 as shown in Fig. 3c. Further increment in NS concentration to 10 % gives extremely highly aggregated particles so that it is difficult to evaluate the particle size from TEM (Fig. 4a). On the other hand, the majority of the size determined using particle size analyzer amounts to 390 nm (Fig. 4b) while the PdI value is equal to 1 and (e) The TEM image in (Figs. 3, 4) shows that St-NPs are significantly larger and darker. This could be attributed to the high concentration leading to overlapping of nanoparticles during the preparation.

It is understandable that high concentration of gelatinized maize starch in aqueous sodium hydroxide solution leads to the formation of highly viscous solution with high retrogradation and gelling tendency of amylose containing starch in addition to its lower water holding capacity [35, 36]. In addition, it was found that increasing the concentration of starch had the major adverse effect on the monodispersity of the nanoparticles. These drawbacks impede penetration of ethanol during precipitation as well as hampers an appropriate diffusion in the NS interior.

It is as well to emphasize that flocculent precipitate is formed because the electrostatic repulsion between St-NPs particles is not sufficient to maintain the stability of these large particles. These data confirm the results observed by TEM and DLS when 7.5 and 10 % NS were used.

On the contrary, utilization of lower NS concentrations (2.5, 5 %) enable to overcome the aforementioned

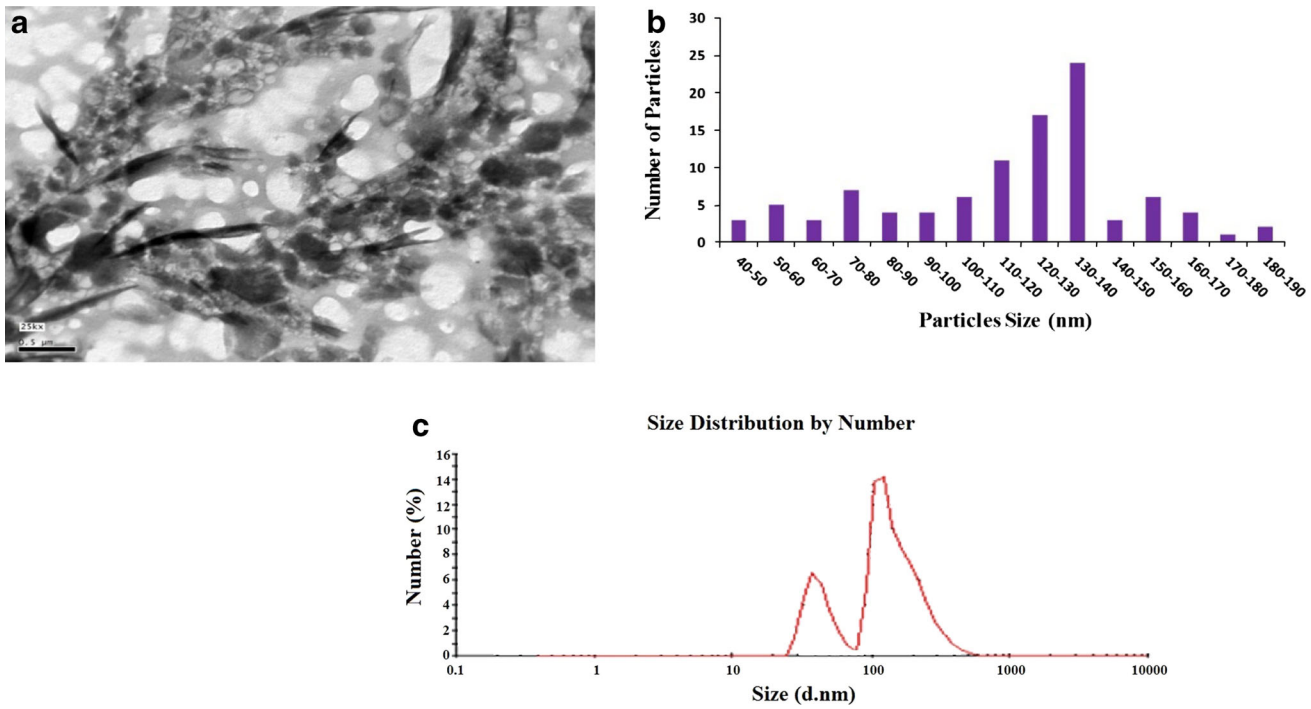

Fig. 1 **a** TEM of St-NPs. **b** Histogram represent the size and size distribution of St-NPs. **c** Particle size analyzer from DLS. Applied conditions: 2.5 g NS, 1.5 g NaOH, total volume 100 ml H_2O; 100 ml absolute ethanol, Temperature 25 °C

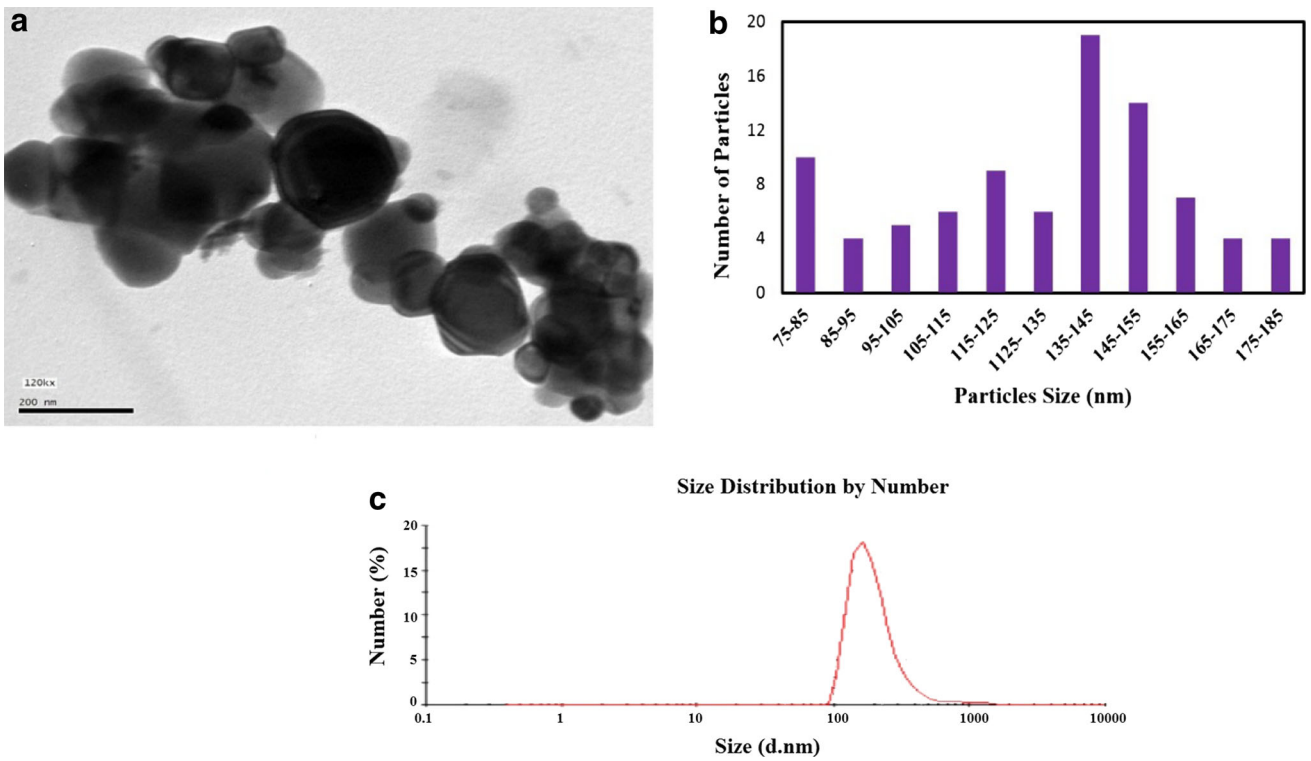

Fig. 2 **a** TEM of St-NPs. **b** Histogram represent the size and size distribution of St-NPs. **c** Particle size analyzer from DLS. Applied conditions: 5 g NS, 1.5 g NaOH, total volume 100 ml H_2O; 100 ml absolute ethanol, Temperature 25 °C

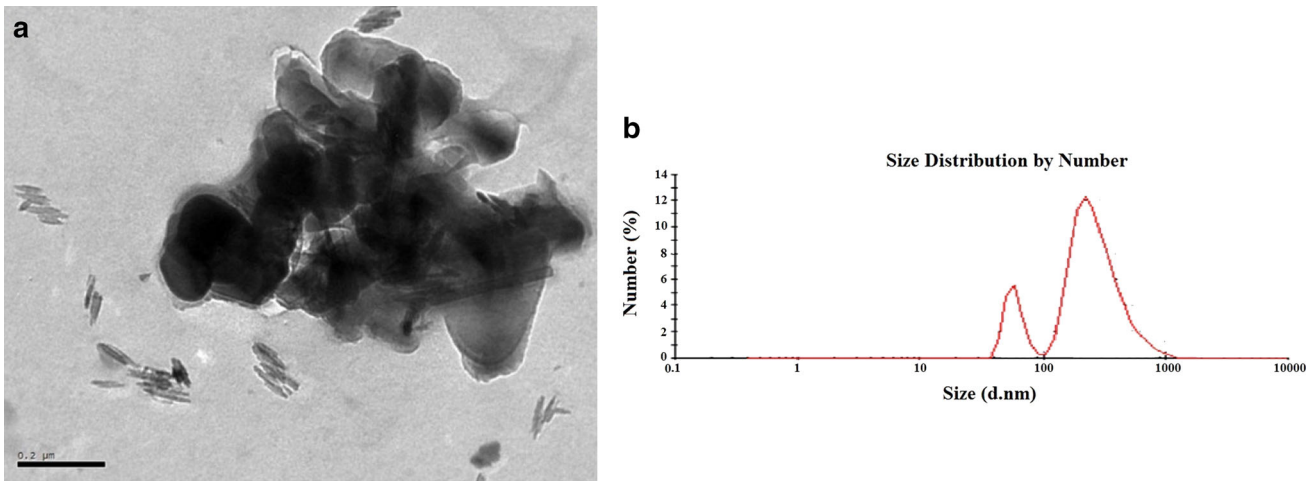

Fig. 3 **a** TEM of St-NPs. **b** Histogram represent the size and size distribution of St-NPs. Applied conditions: 7.5 g NS, 1.5 g NaOH, total volume 100 ml H_2O; 100 ml absolute ethanol, Temperature 25 °C

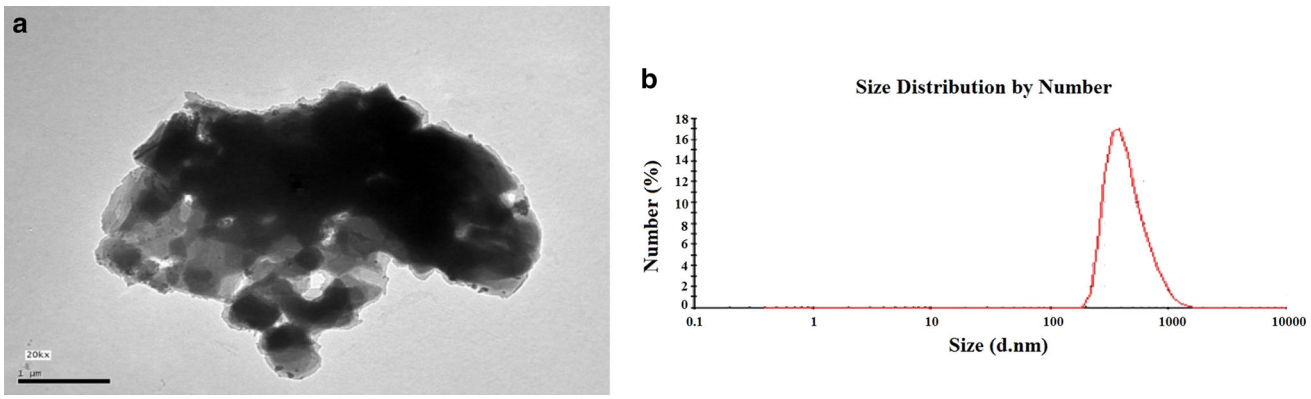

Fig. 4 **a** TEM of St-NPs. **b** Histogram represent the size and size distribution of NPs. Applied conditions: 10 g NS, 1.5 g NaOH, total volume 100 ml H_2O; 100 ml absolute ethanol, Temperature 25 °C

Table 1 Effect of NS concentration on the size and distribution of St-NPs

Formula	NS concentration (%)	Particle size values from TEM (nm)	Majority of particle size from DLS (nm)	PdI
Formula 1	2.5	130–140	132	0.401[a]
Formula 2	5	135–155	164	0.333[a]
Formula 3	7.5	Not determined	220	0.747[b]
Formula 4	10	Not determined	396	1.00[b]

[a] Good quality of the colloidal suspension

[b] Poor quality of the colloidal suspension

shortcomings via formation of gelatinized starch with relatively low viscosity which leads to high dispersion of NS and permits ethanol penetration and formation of St-NPs with reasonable spherical shape and low PdI values (The small PdI value indicate a homogeneous dispersion of St-NPs). This behavior could be explained in terms of the presence of sufficient electrostatic repulsion which causes the stability between St-NPs particles. Table 1 summarizes the effect of NS concentration on the size distribution of St-NPs.

It is seen from Table 1 that the particle size evaluated by DLS was larger than the particle size measured by TEM. This can be traced back to the fact that DLS measures Brownian motion and subsequent size distribution of an ensemble collection of nanoparticles in suspension thereby giving a mean hydrodynamic diameter, which is usually larger than TEM diameter because it represents a dried layer of nanoparticles on a TEM grid. During DLS measurement, there is a tendency of nanoparticles to agglomerate in aqueous state thereby

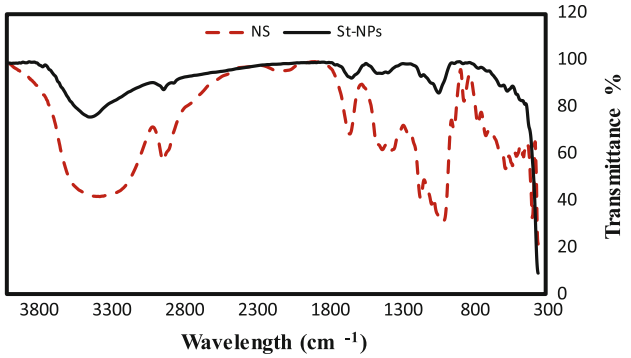

Fig. 5 FT-IR analysis of NS and St-NPs

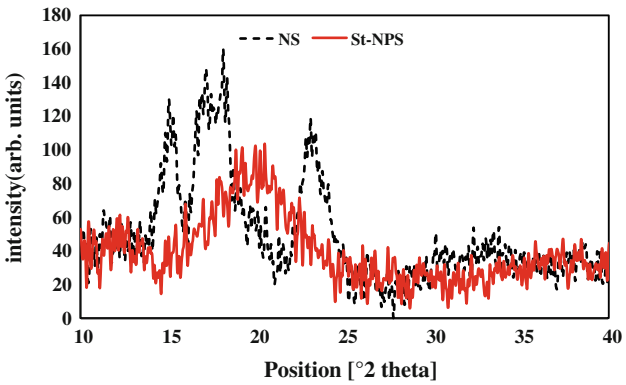

Fig. 6 XRD of NS and St-NPs

giving the size of clustered particles rather than individual particles.

Taking in mind the economical and the yield obtained with respect to the formed St-NPs (Table 1), it could be concluded that using NS concentration 5 % constitutes optimal for the formation of St-NPs with controllable size and PdI.

3.1.1.1 FT-IR Analysis of St-NPs The FT-IR spectra were used to probe the change in the molecular structure after precipitation of starch in the nanoform. The FT-IR spectra shown in Fig. 5 clearly mark the evidence for the presence of starch as revealed by its main characteristic which is represented by a broadband appeared at 3435.7 cm^{-1}; being due to hydrogen bonded hydroxyl group. This broadband is attributed to the complex vibrational stretching associated with free inter and intra molecular bound hydroxyl. The band at 2926.43 cm^{-1} is characteristic of C–H stretching and 1640.1 cm^{-1} due to the stretching and bending vibration of hydrogen bonding O–H groups [37, 38]. Strong absorption band at 1,020 cm^{-1} is due to strengthening of the C–OH bond. The stretching vibration of C–O bonding in C–O–H and C–O–C group in the anhydrous glucose ring appeared at 1150, 1077 and 990 cm^{-1} respectively. The characteristic peak of C–O–C ring vibration in starch located at 760 cm^{-1} [39].

Figure 5 shows that the FT-IR spectra for the freeze-dried St-NPs exhibit almost characteristic bands. In both cases the bands which almost identical with those of FT-IR spectra of NS are dominated by α-1,4-glycosidic linkage and the C–O–C bond in the glucose ring but the strong OH stretching band at 3435.7 cm^{-1} in the NS decreases in intensity when compared with St-NPs due to inter and intra molecular bound hydroxyl groups.

Based on the foregoing, it may be concluded that the preparation of freeze dried St-NPs powder using nano-precipitation technique at room temperature have the same structure of NS without significant fragmentation.

3.1.1.2 XRD investigation for NS and St-NPs Starch is a biopolymer containing semi-crystalline granules with varying polymorphic types and degree of crystallinity. XRD was used to study the change in nano-sized starch particles crystallinity brought about by nano-precipitation of starch molecules dissolved in sodium hydroxide solution. XRD diffraction patterns of freeze-dried St-NPs sample compared to NS are shown in Fig. 6.

As shown in Fig. 6, NS exhibits the A-type diffraction pattern [40] with the peaks at Bragg angles (2θ) at about 15° and 23°, and an doublet at 17° and 18°. The XRD of freeze dried St-NPs exhibits the V-type diffraction peak which was also observed at 20° meanwhile the diffraction peaks at 15°, 17°, 18° and 23° completely vanished [18].

The above findings could be attributed to:

(a) Starch have crystalline structure which means that the particle size of NS is large. In fact, as the particle size decreases, the crystallite size becomes smaller and the diffraction peak becomes broader as shown in the XRD of St-NPs. The width at half height of a peak is inversely proportional to the crystallite size. Also, the disappearance of the diffraction peak appeared in the case of NS may be the consequence of the excessive decrease in the crystallite size arising from the reduction in particle size.

(b) The gelatinized starch formed through dissolution of starch molecules in sodium hydroxide solution followed by the precipitation with absolute ethyl alcohol resulted in disruption of the crystalline structure of clustered amylopectin, apparently leading to nanoparticles with very low intensity and broad amorphous character.

3.1.2 Effect of surfactant concentration on the size distribution of St-NPs fabricated by Solvent displacement technique

Surfactants are found to play an important role in the stability of polymer nanoparticles [41, 42]. Moreover, they

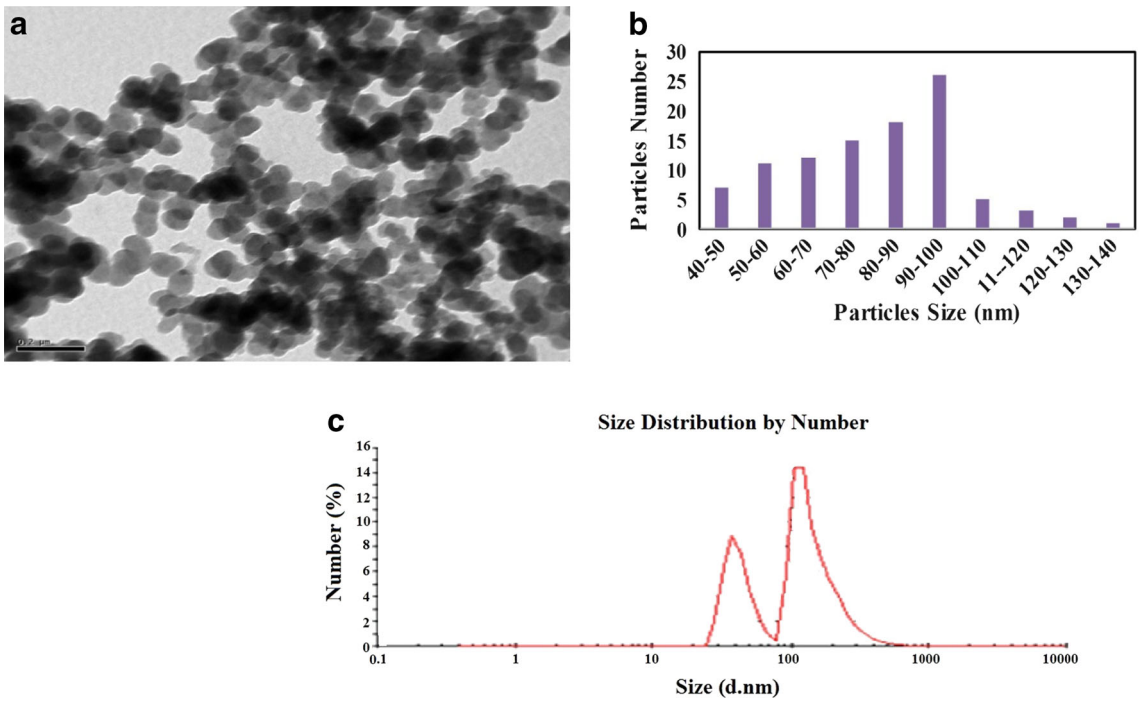

Fig. 7 **a** TEM of St-NPs coated with 10 % (based on weight of NS) Tween® 80. **b** Histogram represent the size and size distribution of St-NPs. **c** Particle size analyzer obtained using DLS. Applied Conditions: 5 g NS, 1.5 g NaOH, 0.5 g Tween® 80, total volume 100 ml; 100 ml absolute ethanol, Temperature 25 °C

increase the surface charge, generate an effective repulsive force between nanoparticles and result in the formation of monodispersed nanoparticle.

Guided by previous reports considering the optimum conditions obtained using 5 % NS; it was decided to use different concentrations of Tween® 80 during the preparation of St-NPs as per the nano-precipitation process. Thus, 5 g of dried NS were added to 80 ml of distilled water containing 1.5 g sodium hydroxide. The alkaline solution containing starch was kept under mechanical stirring for 2 h at 25 °C until formation of homogeneous gelatinized NS. At this end 20 ml distilled water containing different amount of Tween® 80 (10, 20 and 40 % based on weight of NS) were added stepwise to the prepared gelatinized NS and kept under continuous mechanical stirring for another 30 min at 25 °C. Then 100 ml ethanol was added dropwise under vigorous mechanical stirring followed by centrifugation, washing and freeze-drying as described in the experimental section.

The effect of adding surfactant on the particle sizes of the resultant freeze-dried products were monitored using of TEM, particle size distribution obtained from TEM Fig.s and DLS as well as PdI. The results obtained along with their appropriate discuss are given under.

Figures 7, 8 and 9 signify: (i) that addition of 10 % Tween® 80 to the gelatinized NS leads to the formation of St-NPs with small size ranging from 90 to 100 nm (Fig. 7a, b). While the particle sizes evaluated by DLS (Fig. 7c) have a majority size of 112 nm as well as PdI value 0.44; (ii) that increasing the concentration of Tween® 80 to 20 % causes smaller mean size of nanoparticles and the main particle sizes of St-NPs are within the range of 75 and 85 nm (Fig. 8a, b); [43] that the mean particle sizes evaluated by DLS are in a majority of 102 nm and the value of PdI amounts to 0.477 (Fig. 8c); (iv) increasing the concentration of Tween® 80 to 40 % (based on weight of NS) leads to particle sizes with large spherical particles than those obtained with 10 and 20 % and reaches a value of 120–130 nm (Fig. 9a, b). In addition, the mean size investigated by DLS (Fig. 9c) increases and amounts to 141 nm with PdI value of 0.551.

It is logical that Tween-80 is comparatively more hydrophilic and would strongly interact with starch molecules and, in so doings, St-NPs of smaller sizes are precipitated as compared to those of St-NPs prepared in the absence of Tween® 80.

Most probably, presence of surfactants during the precipitation process limits the growth of St-NPs. Once this is the case the observed particles of reduced mean sizes of the St-NPs is affected by the increase in the surfactant concentration. That is why the particle size shows a decreasing trend at 20 % (based on weight of NS) of Tween® 80 when compared with 10 %. Then the particle size exhibits increasing trend at 40 % (based on weight of NS) of Tween® 80.

Interpretation of the above findings can be articulated as follows: the amount of surfactant of 10 % (based on weight

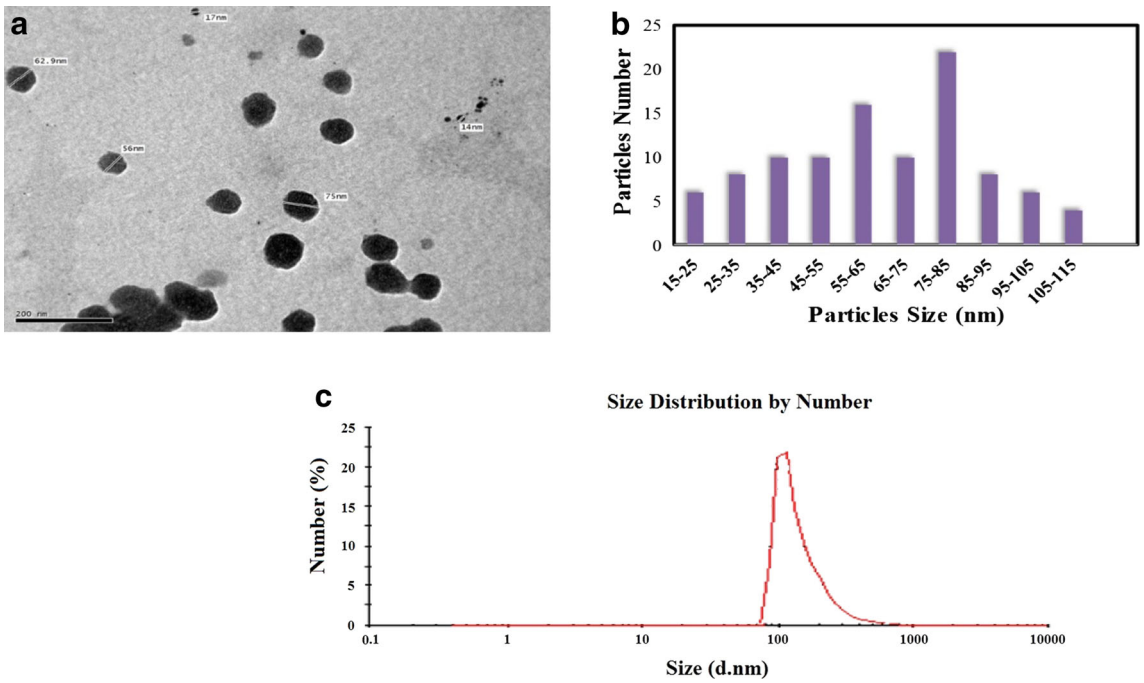

Fig. 8 **a** TEM of St-NPs coated with 20 % (based on weight of NS) Tween® 80. **b** Histogram represent the size and size distribution of St-NPs. **c** Particle size analyzer obtained using DLS. Applied Conditions: 5 g NS, 1.5 g NaOH, 1 g Tween® 80, total volume 100 ml; 100 ml absolute ethanol, Temperature 25 °C

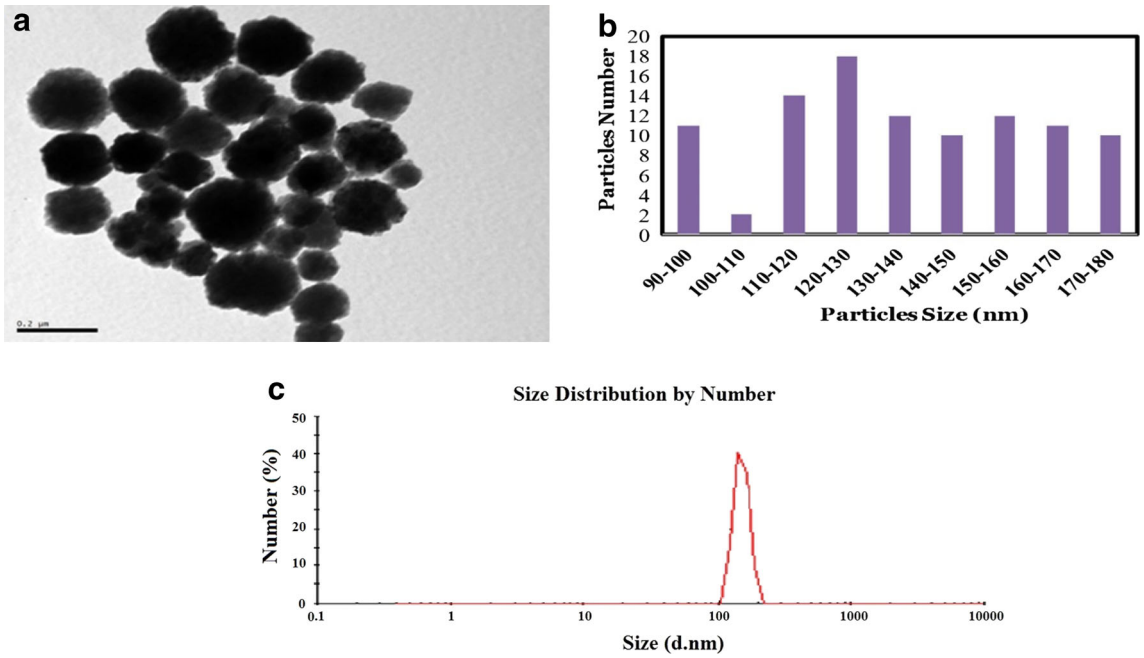

Fig. 9 **a** TEM of St-NPs coated with 40 % (based on weight of NS) Tween® 80. **b** Histogram represent the size and size distribution of St-NPs. **c** Particle size analyzer obtained using DLS. Applied Conditions: 5 g NS, 1.5 g NaOH, 2 g Tween® 80, total volume 100 ml; 100 ml absolute ethanol, Temperature 25 °C

of NS) is not enough to completely coat the entire surface area of the droplets after the homogenization process. Consequently, the droplets tend to aggregate with each other thereby reducing the surface area. On the contrary, when there is an excess concentration of Tween® 80 (40 % based on weight of NS), free emulsifier molecules will be formed within the emulsion, which will ultimately adhere to the droplets, which will be covered by the excess amount

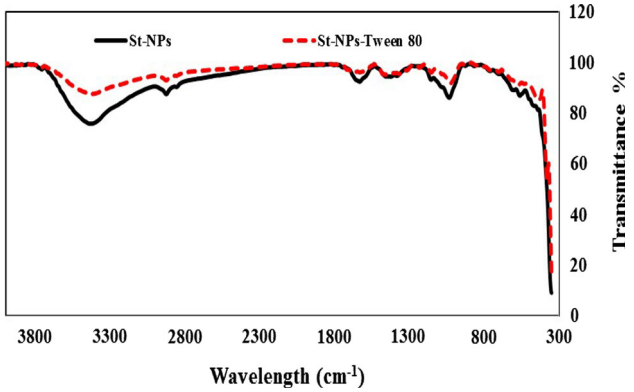

Fig. 10 FT-IR of St-NPs without and with 20 % (based on weight of NS) Tween® 80

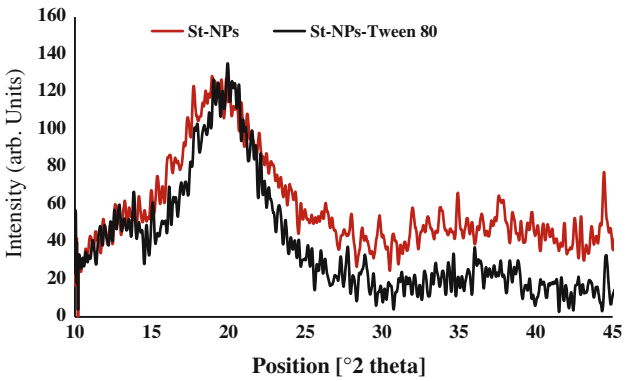

Fig. 11 XRD of St-NPs without and with 20 % (based on weight of NS) Tween® 80

of surfactant. Consequently, the energy available for repelling or pushing the droplets apart decreases and results in increasing the droplets size. This speaks of the permanent importance of right adjustment of the surfactant content and/or determining the optimal amount of surfactant required for optimal coating of the surface of the final droplets.

Obviously, then, the improvement in the spherical particles shape and narrow particle size distribution as monitored by DLS and PdI index because of the addition of different concentration of Tween® 80 in the preparation medium follows the order 20 > 10 > 40 % when St-NPs are fabricated by the nano-precipitation method.

3.1.2.1 FT-IR of St-NPs and St-NPs coated with 20 % Tween® 80 The FT-IR of St-NPs and St-NPs coated with 20 % (based on weight of NS) Tween® 80 are typed in Fig. 10. It is observed that the characteristic absorption bands of St-NPs are the same as those discussed previously in paragraph 3.1.2. The FT-IR of St-NPs coated with 20 % (based on weight of NS) Tween® 80, which acts as stabilizing agent for the formed St-NPs, have the same characteristic bands of St-NPs alone but with low intensity of a broad peak of hydroxyl group which is found at 3,435 cm^{-1}. This broad peak is due to electrostatic reactions formed between hydroxyl groups of St-NPs with polar (head group) hydrophilic part of Tween® 80 indicating that there is no chemical interaction occurring between Tween® 80 and starch molecules.

3.1.2.2 XRD of St-NPs and St-NPs coated with 20 % Tween® 80 Figure 11 shows the XRD of St-NPs coated and uncoated with Tween® 80. The crystallinity of St-NPs is completely different than NS as mentioned above which may be explained as follows. When ethanol was delivered dropwise to starch-paste solution, gelatinized St-NPs were precipitated. Therefore, the gelatinization destroyed A-style crystallinity of NS, which appear at about 15° and 23°, and a doublet at 17° and 18° is completely vanished and hence exhibited the V_H-style crystallinity which appear at 20.8°. The characteristic peak of St-NPS coated with Tween® 80 is nearly similar to that of St-NPs due to the non chemical interaction between St-NPs and Tween® 80.

4 Conclusion

Current work addressed main objective to establish a simple and reproducible method for synthesis of St-NPs. This objective could be fulfilled through modification of the Solvent displacement method by using alkaline aqueous solution as solvent; strong mechanical stirring broke the bonding interaction between starch macromolecules including hydrogen bond in swollen state. In this way, the small particles were split away from each other with the addition of sodium hydroxide solution. In addition, ethanol as precipitant; was added drop-wise to the starch paste solution.

- Characteristics of St-NPs prepared using native starch were performed by making use of world-class facilities. TEM, particle size analyser and PdI confirmed the successful synthesis of spherical St-NPs within the range 135–155 nm with PdI value 0.333.
- FT-IR and X-ray diffractograms signified that the chemical structure of St-NPs have the same structure of the unmodified native starch.
- The optimum conditions for preparation of St-NPs were 5 % NS along with 30 % NaOH based on weight of NS, total volume 100 ml H_2O; 100 ml absolute ethanol, Temperature 25 °C.
- After the addition of 20 % (based on weight of NS) Tween® 80 before precipitation the particle size decreases dramatically to reach a value 103 nm and still in good dispersion.
- The FT-IR and XRD of St-NPs coated with and without Tween® 80 have the same function groups without any

minor shift in the wavelength indicating that there is no chemical reaction between starch and the surfactant.
- It is expected that, the starch in the nanoform will have potential applications in medical domains, particulary or drug carrier.

References

1. M. Ling, W.C. Lin, C.C. Liu, Y.S. Huang, M.J. Chueh, T.S. Shih, J. Hazard. Mater. **83**, 229 (2012)
2. A.K. Gupta, M. Gupta, Biomaterials **26**, 3995 (2005)
3. A. Hebeish, M.E. El-Naggar, M.M.G. Fouda, M.A. Ramadan, S.S. Al-Deyab, M.H. El-Rafie, Carbohydr. Polym. **86**, 936 (2011)
4. M.H. El-Rafie, M.E. El-Naggar, M.A. Ramadan, M.M.G. Fouda, S.S. Al-Deyab, A. Hebeish, Carbohydr. Polym. **86**, 630 (2011)
5. H.A. Silvério, W.P. Flauzino Neto, N.O. Dantas, D.S. Pasquini, Ind. Crops Prod. **44**, 427 (2013)
6. Y. Habibi, L.A. Lucia, O.J. Rojas, Chem. Rev. **110**, 3479 (2010)
7. J.-B. Zeng, Y.-S. He, S.-L. Li, Y.-Z. Wang, Biomacromolecules **13**, 1 (2011)
8. D. LeCorre, J. Bras, A. Dufresne, Carbohydr. Polym. **86**, 1565 (2011)
9. D. LeCorre, E. Vahanian, A. Dufresne, J. Bras, Biomacromolecules **13**, 132 (2011)
10. H. Angellier, J.-L. Putaux, S. Molina-Boisseau, D. Dupeyre, A. Dufresne, Macromol Symp **221**, 95 (2005)
11. S. Chakraborty, B. Sahoo, I. Teraoka, M. Miller Lisa, A. Gross Richard, *Polymer Biocatalysis and Biomaterials*, vol. 246 (American Chemical Society, Washington, 2005)
12. X. Ma, R. Jian, P.R. Chang, J. Yu, Biomacromolecules **9**, 3314 (2005)
13. H. Namazi, F. Fathi, A. Dadkhah, Sci. Iran. **18**, 439 (2011)
14. D.B. Le Corre, J. Bras, A. Dufresne, Biomacromolecules **11**, 1139 (2010)
15. M. Labet, W. Thielemans, A. Dufresne, Biomacromolecules **8**, 2916 (2007)
16. A. Hebeish, M.H. El-Rafie, M.A. El-Sheikh, M.E. El-Naggar, J. Nanotechnol. **2013**, 1 (2013)
17. S.F. Chin, S.C. Pang, S.H. Tay, Carbohydr. Polym. **86**, 1817 (2011)
18. S. Bel Haaj, A. Magnin, C. Pétrier, S. Boufi, Carbohydr. Polym. **92**, 1625 (2013)
19. J.L. Putaux, S. Molina-Boisseau, T. Momaur, A. Dufresne, Biomacromolecules **4**, 1198 (2003)
20. J.Y. Kim, S.-T. Lim, Carbohydr. Polym. **76**, 110 (2009)
21. H. Angellier, S. Molina-Boisseau, M.N. Belgacem, A. Dufresne, Langmuir **21**, 2425 (2005)
22. H. Angellier, L. Choisnard, S. Molina-Boisseau, P. Ozil, A. Dufresne, Biomacromolecules **5**, 1545 (2004)
23. H. Angellier, S. Molina-Boisseau, A. Dufresne, Macromolecules **38**, 9161 (2005)
24. A.M. Shi, D. Li, L.-J. Wang, B.-Z. Li, B. Adhikari, Carbohydr. Polym. **83**, 1604 (2011)
25. D. Liu, Q. Wu, H. Chen, P.R. Chang, J. Colloid Interface Sci. **339**, 117 (2009)
26. F.E. Giezen, R.O. Jongboom, K.F. Gotlieb, A. Boersma, USA. **1** (2004)
27. R.H. Wildi, E.V. Egdob, S. Bloembergen, USA. **1** (2011)
28. U. Bilati, E. Allémann, E. Doelker, Eur. J. Pharm. Sci. **24**, 67 (2005)
29. T. Govender, S. Stolnik, M.C. Garnett, L. Illum, S.S. Davis, J. Control Release **57**, 171 (1999)
30. S. Hyvönen, L. Peltonen, M. Karjalainen, J. Hirvonen, Int. J. Pharm. **295**, 269 (2005)
31. R. Campardelli, G. Della Porta, E. Reverchon, J. Supercrit. Fluids **70**, 100 (2012)
32. H. Fessi, F. Puisieux, J.P. Devissaguet, N. Ammoury, S. Benita, Int. J. Pharm. **55**, 1 (1989)
33. R. Pignatello, N. Ricupero, C. Bucolo, F. Maugeri, A. Maltese, G. Puglisi, AAPS PharmSciTech **7**, 192 (2006)
34. Y. Tao, J. Han, H. Dou, Polymer **53**, 5078 (2012)
35. J. Singh, L. Kaur, O.J. McCarthy, Food Hydrocoll. **21**, 1 (2007)
36. J. Singh, L. Kaur, O.J. McCarthy, in *Advances in Potato Chemistry and Technology*, vol. 273, ed. by S. Jaspreet, K. Lovedeep (Academic Press, San Diego, 2009)
37. S.M. Goheen, R.P. Wool, J. Appl. Polym. Sci. **42**, 2691 (1991)
38. K. Lammers, G. Arbuckle-Keil, J. Dighton, Soil Biol. Biochem. **41**, 340 (2009)
39. M. Černá, A.S. Barros, A. Nunes, S.L.M. Rocha, I. Delgadillo, J. Čopíková, M.A. Coimbra, Carbohydr. Polym. **51**, 383 (2003)
40. H.F. Zobel, in *Methods in Carbohydrate Chemistry*, vol. 109, ed. by L.R. Whistler (Academic Press, New York, 1964)
41. J.P. Rao, K.E. Geckeler, Prog. Polym. Sci. **36**, 887 (2011)
42. G. Gotchev, T. Kolarov, K. Khristov, D. Exerowa, Adv. Colloid Interface Sci. **168**, 79 (2011)
43. J.O. Winter, M. Gokhale, R.J. Jensen, S.F. Cogan, J.F. Rizzo III, Mater. Sci. Eng. C **28**, 448 (2008)